Journal of Physics: Conference Series **755** (2016) 012002 doi:10.1088/1742-6596/755/1/012002

Development and calibration of a MFM-based system for local hysteresis loops measurements

M. Coïsson, G. Barrera, F. Celegato, P. Tiberto
INRIM, strada delle Cacce 91, 10135 Torino (TO), Italy

E-mail: m.coisson@inrim.it

Abstract. A measurement technique derived from a field-dependent magnetic force microscope (MFM) is presented for the measurement of local hysteresis loops on patterned micrometric and sub-micrometric magnetic structures. The technique exploits the synchronisation of the applied field variations with the end-of-line signal of the microscope, while keeping the slow scan axis disabled. In this way, a single MFM image contains the whole field evolution of the magnetisation processes in the sample along a user-defined profile. An analysis procedure is presented for the subsequent determination of local hysteresis loops on magnetic dots. The system has been calibrated for what concerns the applied field values. No significant artifacts induced in the measurements by the applied field have been observed up to applied fields of $\approx$ 1000 Oe.

1. Introduction

In recent years, the need has emerged to reliably measure the physical properties of materials at the micrometer or sub-micrometer scales exploited by the new lithographic techniques available in nanotechnology [1, 2]. Among the important properties that need to be investigated, magnetisiation processes as a function of the applied magnetic field in patterned magnetic structures are of utmost importance in a variety of applications, including magnetic recording, spintronics, sensors [3]. However, available magnetometry techniques, including high-sensitivity SQUIDs, or optical Kerr-effect microscopes, lack the required sensitivity to investigate individual patterned structures or space resolution respectively [4, 5]. Therefore, the solution so far has been to investigate large arrays of nominally identical structures in order to overcome these limitations. Experimental techniques such as SEMPA are actually able to provide access to the sub-micrometer scale on magnetic samples, but are not widely available [6].

Magnetic force microscopy (MFM) is a technique that offers excellent space resolution but limited possibility of investigating the magnetic-field dependence of the magnetisation of the sample [7, 8, 9, 10, 11]. In fact, each MFM image is quite time-consuming, and it is not possible to acquire hundreds of images of the same sample at different applied magnetic fields with a single tip. Recently, an MFM-derived setup has been presented [12] that overcomes this limitation by allowing the acquisition of a single magnetic image, made of several hundreds of lines, each acquired at a different applied magnetic field. In order to achieve this result, a single profile of the measured patterned structure is repeatedly acquired as a function of the applied field; from this information, the magnetisation evolution of the whole patterned structure is inferred, therefore providing a convenient way to measure "local hysteresis loops" on patterned magnetic systems with a widely available setup.


Content from this work may be used under the terms of the Creative Commons Attribution 3.0 licence. Any further distribution of this work must maintain attribution to the author(s) and the title of the work, journal citation and DOI.
Published under licence by IOP Publishing Ltd

In this paper, on overview of this technique is presented, with particular emphasis on the development of the experimental setup and on its calibration. Examples of local hysteresis loops on $Ni_{80}Fe_{20}$ dots with a lateral size of 2μm are reported.

2. MFM-based local field loops measurement setup

A system aimed at the measurements of local hysteresis loops based on a magnetic force microscope (MFM) has been developed. The selected microscope (a Bruker Nanoscope V Multimode 8) is equipped with a fully non magnetic scanner, head and tip holder, and is coupled with an electromagnet surrounding the head. The sample is located in the geometrical centre of the magnet, whereas the Hall probe used for the measurement of the applied magnetic field is placed close to one of the poles. The difference between the measured field and its value at the position of the sample will be taken into account with a suitable calibration procedure discussed in the following section. The field is applied in the sample plane along the direction of the fast scan axis.

In order to measure local hysteresis loops, the procedure summarised in [12] is discussed here in more details. A patterned magnetic sample, i.e. a $Ni_{80}Fe_{20}$ dot with a lateral size of 2μm and a thickness of 30 nm, is imaged with the microscope in intermittent contact mode, while the magnetic signal is acquired in lift mode using the phase channel. An AFM representation of a selected dot is shown in Fig. 1. A profile of the dot is arbitrarily chosen, to be repeatedly scanned by disabling the slow scan axis of the microscope. In Fig. 1 an example of a possible choice of scanned profile is shown by the dashed line.

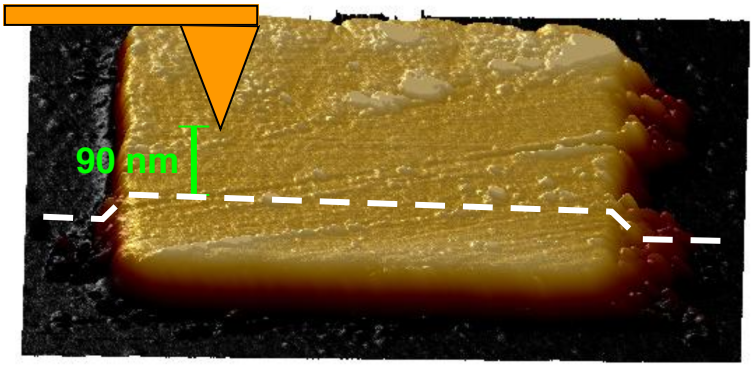

Figure 1. 3-dimension atomic force microscopy image of a $Ni_{80}Fe_{20}$ dot with a lateral size of 2μm and a thickness of 30 nm. The dashed line represents a profile that is repeatedly scanned during local hysteresis loops measurements. The tip is also schematically drawn indicating the lift scan height at which MFM data is acquired.

The field-dependence of the magnetisation of the dot can be obtained by submitting the sample to a different magnetic field intensity each time the same profile is acquired. In order to achieve this result, the end-of-line (EOL) signal of the microscope controller is processed by custom electronics, whose diagram is shown in Fig. 2. This electronic circuit counts the transistor-to-transistor logic (TTL) impulses that the MFM controller sends each time the tip has finished scanning a line. Since the magnetic signal is acquired in pass 2, the microscope sends 2 EOL signals for each repetition of the profile scansion, one for the height channel (AFM data) and one for the phase channel in pass 2 (MFM data). The electronic circuit counts the impulses and sends the result to a control PC that communicates through a RS232 interface. In this way, the control PC can synchronise the variations of the applied magnetic field with the

EOL signals, ensuring that each time the dot profile is acquired, a new value of the magnetic field is applied and is stable throughout the whole acquisition process.

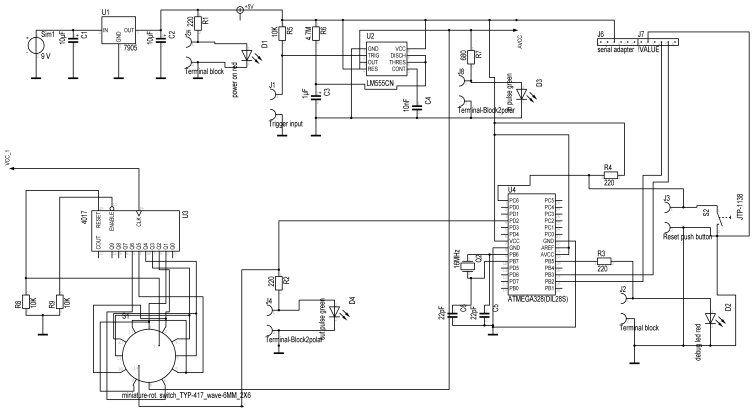

Figure 2. Circuit scheme of the custom electronics used count the EOL signals of the MFM controller and communicate with the control PC.

Figure 3 shows an example of local hysteresis loop acquisition on a profile similar to the one marked in Fig. 1 with the dashed line. In panel (a), the morphology (height channel, pass 1) is reported; as the slow scan axis is disabled, the same profile is repeatedly acquired until the whole frame is filled. The dashed lines clearly mark the dot edges, indicating a negligible drift during the scanning. As each line is acquired, the magnetic field changes, resulting in the MFM signal (phase channel, pass 2) shown in Fig. 3(b). In this case, the resulting image is no longer independent on the line, as in panel (a), because the magnetic signal is affected by magnetisation structure in the dot, that reflects the variations of the applied magnetic field. In panel (c), in false colours, the applied magnetic field is reported: it can be seen that after the acquisition of a few lines at the top of the image, the field is suddenly switched on at its maximum value, then gradually decreased through zero down to the minimum value, and then back again to its initial value. The last third of the figure in panel (c) shows that the field has been switched off. The same information is reported in panel (d), but with an indication of the actual field values. The field dependence in Fig. 3(d) is actually just a vertical profile along Fig. 3(c). The switching off of the field at the end of the hysteresis loop is clearly visible in the MFM signal, and very weakly visible in the height channel.

Figure 3 has been obtained by choosing a profile close to an edge of the dot; however, this choice is not critical, as in principle any profile could be picked up to measure local hysteresis loops. Indeed, the choice should be driven by the amount of information that can be extracted from the MFM image along the acquired profile. In the case of a magnetic dot displaying a vortex magnetisation at the remanence, a profile close to the symmetry axis of the dot (i.e. passing through its centre) is not particularly indicated, as relatively weak phase variations occur as a function of the applied field; therefore, a profile closed to a dot edge has been chosen, but it is not necessary to precisely know its position.

3. Calibration and validation

Before analysing Fig. 3, it is necessary to perform a few validation steps. As discussed in Section 2, the Hall probe used for measuring the field is placed close to a magnet pole, and not to the sample that is located in the centre of the gap. It is therefore required to calibrate the magnetic field in order to apply the calcuated correction factor to the signal displayed in Fig. 3(c). To this purpose, two Hall probes have been used during the calibration process, the second one

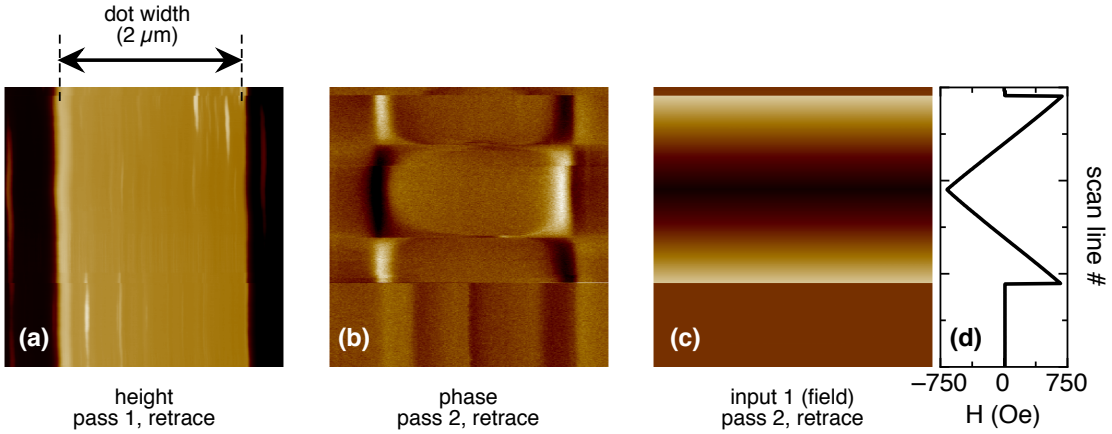

Figure 3. (a) Dot profile acquired with the height channel with the slow scan axis disabled. The dashed lines mark the dot edges. (b) Corresponding MFM image (phase, pass 2) at a lift scan height of 90 nm. (c) Applied magnetic field (in false colours) as a function of the acquired scan line. (d) Same as (c), in Oe.

being positioned at variable distance from a magnet pole, without the microscope head. As the head is totally non magnetic, it has no shielding effect and can be safely removed to perform the field calibration. The results are displayed in Fig. 4, where the difference between the two probes readings is reported as a function of $H_{nominal}$ (the field measured by the Hall probe close to the magnet pole and used during the experiments) and of the distance of the second probe with respect to the same magnet pole.

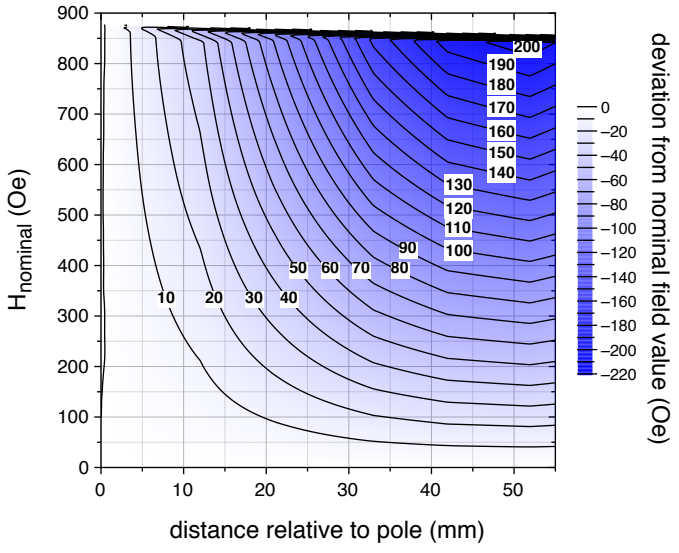

Figure 4. Difference between the magnetic field measured by the Hall probe close to the magnet pole ($H_{nominal}$) and the one measured by the second Hall probe (contour and colour plots and labels) as a function of $H_{nominal}$ and of the distance of the second Hall probe with respect to a magnet pole.

The contour plots shown in Fig. 4 indicate that at ≈ 52 mm from the pole (where the sample is located) the deviation between the two field measurements has a significant dependence on the

second probe position especially at high applied field values. As a consequence, it is important to place the magnet around the head as much as possible always in the same position. Conversely, as the sample only moves by a few tens of micrometers during scanning in the microscope, its movement is not critical for the determination of the actual magnetic field. The final calibration curve applied at the ≈ 52 mm position is reported in Fig. 5, that can be used to calculate the actual field value in the magnet centre (where the sample is located), for any given nominal magnetic field measured by the probe close to the magnet pole.

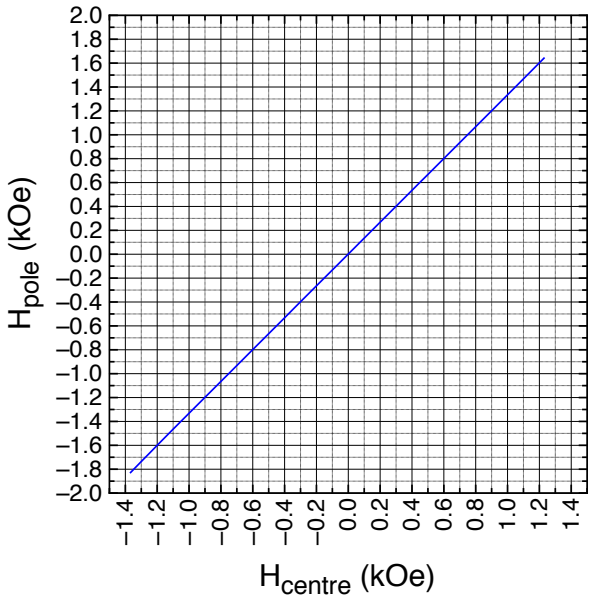

Figure 5. Relationship between the actual field value at the centre of the magnet and the value measured by the Hall probe close to one of its poles.

The field values reported in Fig. 3(d) have already been rescaled from the raw data of Fig. 3(c) according to the calibration curve of Fig. 5.

Even though the microscope head, scanner and tip holder are not magnetic, the tip used for MFM imaging is of course coated with a magnetic material, and its response to an applied magnetic field has to be investigated, as spurious effects may lead to misinterpretation of the magnetic data. MFM tips usually report nominal coercivity values that refer to the field that is necessary to reverse their magnetisation along their axis. In our setup, the magnetic field is applied along the sample plane, i.e. perpendicular to the tip axis. Even in this case, it is safer to choose a tip whose nominal coercive field is larger than the maximum applied field. In our case, we opted for Co-Cr coated HR-MESP tips whose coercivity is ≈ 900 Oe. The absence of artifacts in MFM images induced by the application of an in-plane magnetic field has been verified with a Cu sample displaying a sharp step. The results, obtained with the same procedure exploited for the data reported in Fig. 3, are shown in Fig. 6.

As it can be seen in Fig. 6(b), the magnetic signal does not show any dependence on the applied field; it has to be remarked that the image is more noisy than Fig. 3(b) because, being the imaged sample non magnetic, the phase variations are much more limited and the colour scale is much more magnified; this further supports the absence of artifacts induced in the MFM image by the applied field. As a consequence, the phase data obtained in Fig. 3(b) can be considered reliable and further analysed to investigate the magnetisation reversal processes occurring in the studied dot. A further proof that the application of the in-plane magnetic field has not significantly perturbed the tip is given by the fact that when the field is switched off the

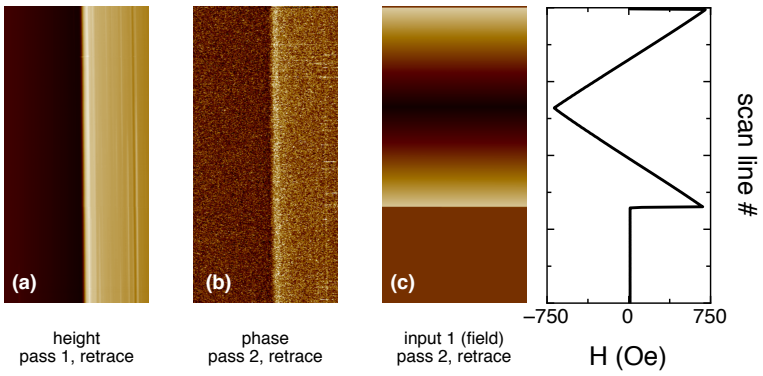

Figure 6. Height, MFM and field profiles of a Cu sharp step as a function of the applied magnetic field.

magnetic contrast is not lost (see bottom of Fig. 3(b)): if the tip magnetisation had flipped out of its axis during the application of the field, the magnetic contrast would have been lost since the microscope is operated in the normal vertical oscillation of the cantilever, that is sensitive only to the second derivative of the vertical component of the magnetic field generated by the underneath magnetisation of the sample along the vertical direction, provided that the tip is magnetised along the same axis.

In order to proceed with the investigation of the reversal processes occurring in the studied dot, the MFM signal reported in Fig. 3(b) must be analysed as a function of the applied field (Fig. 3(c) and (d)). To this purpose, the procedure described in Fig. 7 is applied.

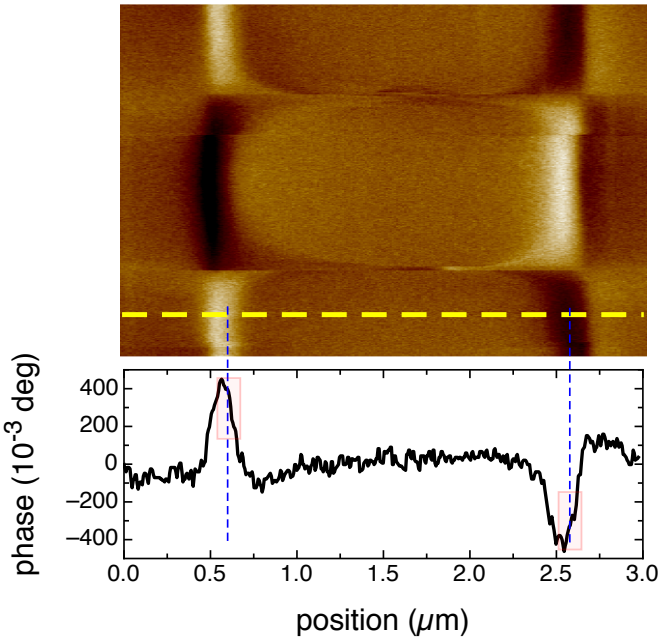

Figure 7. Top: same as Fig. 3(b). Bottom: phase profile along the yellow dashed line. The blue dashed lines indicate the positions of the left and right dot edges. The shadowed areas mark the data that have been used for the analysis described in the text.

Each line of the MFM image is extracted and the two dot edges are identified: this information is available through the height channel that is simultaneously acquired. Then, a subset of the phase data is extracted around the position of the two dot edges, with a lateral size of a few tens of nanometers. The phase signal is then averaged independently for each of the two selected portions of the line (shaded areas in Fig. 7), and the two results subtracted. In the end, for each line of the MFM image a "phase contrast" value is obtained, being e.g. positive for the line reported in Fig. 7 and negative when the dominant colour close to the dot edges is reversed. The "phase contrast" can then be plotted as a function of the applied field, resulting in the so-called "local hysteresis loop", shown in Fig. 8.

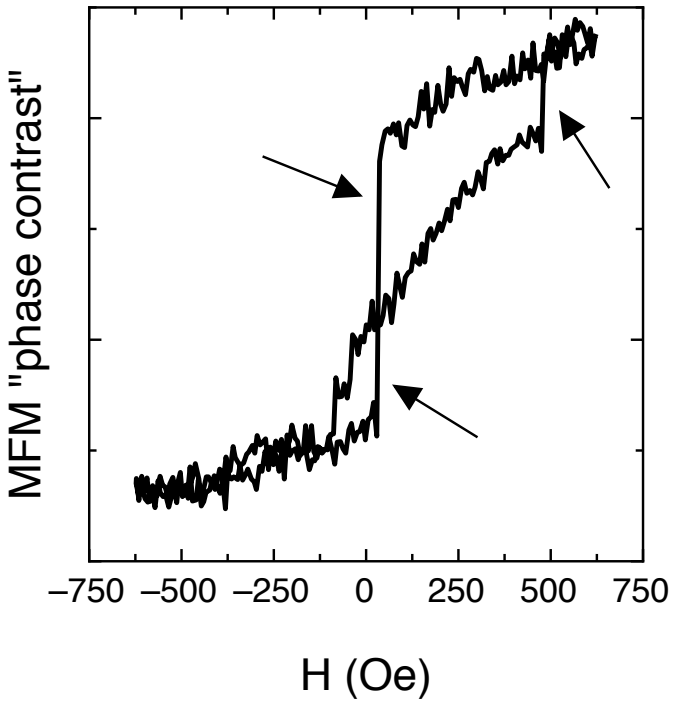

Figure 8. Local hysteresis loop of the $Ni_{80}Fe_{20}$ dot having a side of 2μm and a thickness of 30 nm. The arrows indicate irreversible features in the magnetisation reversal processes.

The curve displayed in Fig. 8 reports, in the vertical axis, the "phase contrast", that is expressed in arbitrary units since the response of the MFM tip has not been calibrated to a traceable standard giving a reference value of the field gradient to which the tip is sensitive. However, should a quantitative measurement be required, such calibration can be performed as described in [13, 14, 15]. In our case, it is not necessary to know the magnetisation value of the dot, as our interest lies in the mechanisms induced by the varying magnetic field. These are clearly visible in Fig. 8 in the form of abrupt jumps marked by the arrows. A suitable comparison with micromagnetic simulations allows to unequivocally assign these jumps to irreversible magnetisation processes occurring in the dot, in the form of magnetic vortex nucleation and expulsion [12]. These field values can be obtained with other experimental techniques, but magnetometers (e.g. SQUID) require rather large arrays of identical and non interacting dots, whereas magneto-optics setups do not have the space resolution to distinguish the details of the magnetisation patterns in structures having sizes smaller than $\approx 1 - 2\mu$m. Conversely, the present MFM-derived setup provides both space and field resolution required for the investigation of magnetisation reversal processes in micrometric and sub-micrometric

individual patterned structures.

4. Conclusions

An experimental setup for the measurement of local hysteresis loops on micro-and nanometric patterned structures, based on a field-dependent magnetic force microscope, has been presented and calibrated. The setup allows to image the magnetic field evolution of the magnetisation in a patterned system (e.g. a magnetic dot) by acquiring a single MFM profile as a function of the applied field. A suitable image analysis, exploiting the "phase contrast" at the patterned structure edges, provides access to all the relevant irreversible magnetisation reversal processes that occur in the sample. The system has been properly calibrated for what concerns the accurate field values applied to the sample. Conversely, the proposed setup does not require calibration of the response of the MFM tip, unless a quantitative measurement of the sample magnetisation is required. The presented data support a field-dependent response of the technique that is sensitive to the variation of the magnetic properties of the sample without significant artifacts up to applied field of ≈ 1000 Oe.

Acknowledgments

This work has been partially performed at NanoFacility Piemonte, an INRIM laboratory supported by Compagnia di San Paolo.

References

[1] *Nanoelectronics and information technolgy: Advanced electronic materials and novel devices*, R. Waser ed., Wiley-VCH, Weinheim (2003).
[2] *Magnetic nanostructures*, H.S. Nalwa ed., American Scientific Publishers, USA (2002).
[3] *Nanomagnetism and Spintronics*, T. Shinjo ed., Elsevier (2009).
[4] H.J. Williams, F.G. Foster, E.A. Wood, Phys.Rev. **82** 119 (1951).
[5] D.A. Allwood, G. Xiong, M.D. Cooke, R.P. Cowburn, J. Phys. D: Appl. Phys. **36** 2175 (2003).
[6] M.R. Scheinfein, J. Unguris, M.H. Kelley, D.T. Pierce, R.J. Celotta, Rev. Sci. Instrum. **61** 2501 (1990).
[7] U. Hartmann, J. Magn. Magn. Mater. **157** 545 (1996).
[8] P. Grütter, H.J. Mamin, D. Rugar, *Magnetic force microscopy (MFM): Scanning Tunneling Microscopy vol 2*, H.-J. Güntherodt and R Wiesendanger ed, Springer, Berlin, pp 151-207 (1992).
[9] T.G. Sorop, C. Untiedt, F. Luis, M. Kroll, M. Rasa, L.J. de Jongh, Phys. Rev. B **67** 014402 (2003).
[10] M.V. Rastei, R. Meckenstock, J.P. Bucher, Appl. Phys. Lett. **87** 222505 (2005).
[11] M. Jaafar, L. Serrano-Ramón, O. Iglesias-Freire, A. Fernández-Pacheco, M.R. Ibarra, J.M. DeTeresa, A. Asenjo, Nanoscale Res. Lett. **6** 407 (2001).
[12] M. Coïsson, G. Barrera, F. Celegato, E. Enrico, A. Manzin, E.S. Olivetti, P. Tiberto, F. Vinai, J. Phys. D: Appl. Phys. **47** 325003 (2014).
[13] L. Kong, S.Y. Chou, Appl. Phys. Lett. **70** 2043 (1997).
[14] P.J.A. van Schendel, H.J. Hug, B. Stiefel, S. Martin, and H.-J. Güntherodt, J. Appl. Phys. **88** 435 (2000).
[15] T. Göddenhenrich, H. Lemke, M. Mück, U. Hartmann, C. Heiden, Appl. Phys. Lett. **57** 2612 (1990).